Mech. Adv. Technol., Vol. 8, No. 4, 2024, pp. 428–440

DOI: 10.20535/2521-1943.2024.8.4(103).313412

UDC 539.3

Numeric analysis of elastic plane body static problem by the method of matched sections

Kirill Danylenko[1] • **Igor Orynyak**[2]

Received: 8 November 2024 / Revised: 3 December 2024 / Accepted: 16 December 2024

Abstract. *The paper continues the series of authors' works on the elaboration of a principally new variant of the finite element method, FEM, for the treatment of various problems of mathematical physics, namely the method of matched section, MMS. The elastic plane body under static loading is considered here. As in FEM, the whole body is meshed into the small elements of, preferably, rectangular form. The main peculiarity of the method consists in the introduction of a set of main parameters dependent only on one coordinate variable, i.e. either x or y. So, any differential equilibrium equation with two partial derivatives concerning x or y is broken out into two relatively simple equations concerning only one independent variable. This leads to the introduction of one additional constant showing the interchange between these two equations. The introduced constants can be derived from the equation of continuity of kinematic parameters in the center of each element. The main, for example, x-dependent parameters are: $v^x(x)$ and $u^x(x)$ displacements in vertical $(y-)$ and horizontal $(x-)$ directions, respectively; normal $N^x(x)$ and tangential (shear) $L^x(x)$ forces in x direction, and y direction, respectively; and bending moment $M^x(x)$ and angle of rotation $\theta(x)$. Similar parameters are established for y-direction. Based on the methodology of the transfer matrix method the analytical matrix-form dependence between these parameters in any point x or y and those at the lower and/or left border of the element are established. For the treatment of oblique and curvilinear boundaries, the right triangular element as a special degenerate case of the rectangular element is derived. The resulting system of linear equations is formulated for unknown values of all parameters specified at the border of all elements. The efficiency and the superb accuracy of the MMS are demonstrated in the classical examples of bending of a long rectangular body (beam-like geometry) and tension at infinity of a 2D body with a small circular hole.*

Keywords: *method of matched sections, transfer matrix method, elastic plane body, triangular element, boundary conditions, plate with a circular hole.*

1. Introduction

The paper is a further development of the method of matched section, MMS, [1]–[4] as a new branch of finite element method, FEM, in application to plane body problem. Like FEM it supposes that the whole domain is represented as a mesh of simple elements; algebraic relations between main physical and geometrical parameters are established from the governing differential equations; these relationships are compiled locally for all elements and then assembled into one global matrix.

✉ K. Danylenko
k.a.danylenko@gmail.com

✉ I. Orynyak
igor_orinyak@yahoo.com

[1] *Igor Sikorsky Kyiv Polytechnic Institute, Kyiv, Ukraine*

Nevertheless, MMS has the following distinctive features:

A) It explicitly operates by all geometrical and physical parameters of the considered problem, rather than, say, by displacements through which all others are expressed. The unknowns are prescribed to the central line between two opposite sides of the element, rather than to its vertices (nodes) as in FEM. They are equally important in the compilation of a global matrix of equations. The matrix coefficients result from approximate analytical solution of all 1D differential equations, instead of minimization of some functional or residual.

B) Analytical solutions are reduced to the solution of a set of ordinary 1D differential equations concerning each local independent variable. If the governing equilibrium equation is the partial differential equation with respect to 2 (in 2D case) independent variables (x and y), then it is broken out into two ordinary differential equations each

concerning either of x or y variable with introducing one additional unknown constant for accounting the interaction between them. This constant will be further determined through the supplemental requirement of continuity of geometrical parameters in the element center. The 1D analytical solutions (connection equations) within each element are written in the form of a transfer matrix between inlet and outlet parameters, where the unknowns at the left and lower sides of the element are considered as the inlet and those at the upper and right sides – as the outlet ones.

C) The continuity conditions (conjugation equations) between different elements are provided at the sides of the neighboring elements by equating all corresponding governing parameters. Another significance of them consists in the possibility to introduce the outer force between them, imposed jumps of kinematic parameters.

It is often argued that FEM is strictly based on the minimization procedure for weighted residuals or some functional. We think that it is not so. Early development of FEM was based on a matrix structural analysis which completely stemmed from the analogy with the beam and rod behavior [5], [6]. Furthermore, in explaining the essence of FEM the authors of famous textbooks often say that the goal of the auxiliary minimization procedure is to get similar relations between the kinematic and force parameters in 2D and 3D cases similarly as in the known solutions for beams and rods [7].

For 1D structures, the same (exact or approximate) analytical solution can be considered as a foundation for either FEM (or stiffness method) or transfer matrix method. The difference is in the way of presentation of the solution matrix [8], [9]. If the dependencies are given as those between the inlet (left side) and outlet parameters, then we have the transfer matrix method solution [9]–[12]. If the force parameter on the left and right sides are expressed through left and right sides kinematic parameters, then the FEM (or stiffness method) is to be applied [14]–[16].

Employment of analytical solutions in MMS has another obvious advantage. One always can guess what to expect from the method: its accuracy, means, and phenomena to be addressed. For example, if some parameter or effect is accounted for in the analytical solution it always would lead to predictable output results without any locking effects or artificial loss of stability. For example, if the shear deformation is explicitly included in the governing differential equations, then the solution will never exhibit the shear locking, and for the small thickness-to-length plate ratio it will converge to the thin plate results [1].

The primary requirement for MMS is that it is constructed in such a way that equilibrium equations are exactly satisfied on the boundary of the element. Considering that they exactly match on the borders between elements, one can conclude that equilibrium is fulfilled for the whole body too. The requirement for keeping the equilibrium is the most important in mechanics ("Equilibrium is Essential, Compatibility is Optional" [17]). Yet most commercial software does not provide the fulfillment of this requirement [18], so alternative FEM approaches which keep the equilibrium at the sides between the neighboring elements are recently intensively developed within hybrid or mixed formulations [18]–[20]. So, MMS satisfies recent trends in computational mechanics.

MMS can be easily enhanced by the employment of more sophisticated physical models and their solutions as connection equations. An example is the transient heat conduction analysis by MMS where the connection equations contain the time step as a model parameter [3]. In that work [3], it realizes 2D geometry the Bathe's idea that basic functions within an element could be time-dependent ones [21], [22]. A similar enhancement within MMS was made for the plate transverse vibration analysis [4], where the solution was given with explicit accounting for the unknown natural frequency, so the solution was derived as the 2D spectral one.

This work is restricted to the elastic plane body static analysis. The main goal is to show the applicability of the MMS to this problem, where MMS has the same salient features as in previous applications – it allows to use the drastically different ratio of properties and dimensions. Contrary to work [1] the technical emphasis is made on the development of the right triangular element with the ability to account for its deformation with subsequent analysis of the curvilinear boundaries.

2. Differential equations for the 2D plane body

The peculiarity of the proposed solution is that all partial differential equations are not combined to form one governing equation. They are to be considered individually. On the other hand, in contrast to the transverse plate problem [1] where all equations are already written in the textbooks in the beam-like digestible form, here we need to reformulate the governing differential equations in a similar beam-like manner for two different directions.

2.1. Main parameters and notions

The classical plane problem operates by two displacements and three stresses. Following the general beam-like methodology we introduce here 6 main parameters on each side of the element, Fig 1. Take the rectangular element of length a (along the x-*axis*), and height b (along the y-axis) as the basic geometrical element of the analysis. Introduce the local coordinate system originated at the left-lower edge, Fig 1. Let us consider the element as if it were formed by two perpendicular beams – one in *the* x direction (x-beam) and the other one in *the* y direction (y-beam). Introduce the set of main notions and parameters. Note, that upper indexes "x" or "y" characterize the sides (or another word – the beams) they are related to, while for parameters shown in Fig 1 the lower index "0" means that it pertains to the origin of a "beam".

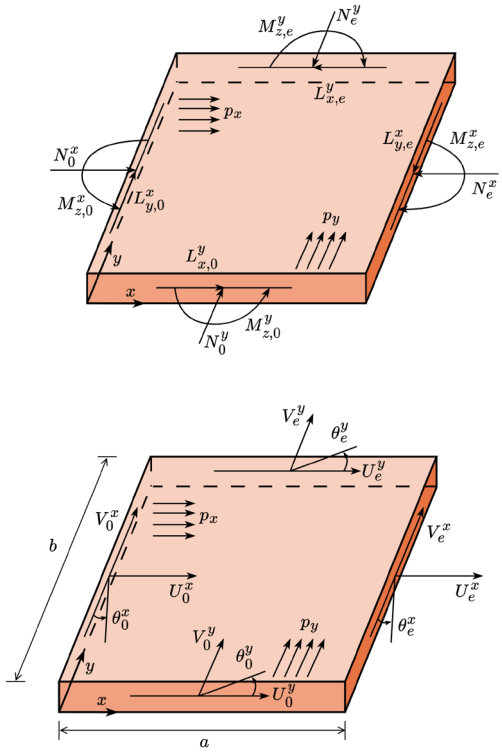

Fig 1. The scheme and designations for a rectangular element

Start from x-beam. It is characterized by 6 governing scalar parameters. They are related to the central line along the x direction, i.e. to $y = b/2$, and are the following, Fig 1:

– Vectorial concentrated force $\vec{F}^x(x)$ which consists of two scalar components: normal force $N^x(x)$ (acting in x direction) and tangential (shear) force $L^x(x)$ (directed toward y-axis), Fig. 1, i.e.:

$$\vec{F}^x(x) = N^x(x)\vec{i} + L^x(x)\vec{j} \tag{1a}$$

– Scalar (in this problem) bending moment $M_z^x(x)$ acting against the clockwise direction (i. e. around the third z direction).

– Vectorial uniform displacement $\vec{\Pi}^x(x)$ which consists of two scalar components: normal displacement $u^x(x)$ (acting in x direction) and tangential one $v^x(x)$ (directed toward y-axis), i.e.:

$$\vec{\Pi}^x(x) = u^x(x)\vec{i} + v^x(x)\vec{j} \tag{1b}$$

– Scalar (in this problem) rotation angle $\theta_z^x(x)$ rotating against the clockwise direction (i.e. around the third z direction).

Note, that axial force $N^x(x)$ and bending moment $M_z^x(x)$ produce compressive axial stresses, $\sigma^x(x,y)$ at each side $x = const$:

$$\sigma^x(x,y) = \sigma_N^x(x) - \frac{2\left(y - \frac{b}{2}\right)}{b} \cdot \sigma_M^x(x), \tag{2a}$$

where stress components are given by formulas:

$$\sigma_N^x(x) = \frac{N^x(x)}{tb}; \quad \sigma_M^x(x) = \frac{6 \cdot M_z^x(x)}{tb^2}, \tag{2b}$$

where t is the plate thickness; usually we take it to be 1. Shear force $L^x(x)$ produces uniform shear stress at this side:

$$\tau^y(x) = \frac{L^x(x)}{tb} \tag{2c}$$

Now consider the displacements along the side $x = const$. Everything is clear about the displacement $v^x(x)$ in the tangent $(\vec{j})$ direction. In contrast, the displacement in the normal $(\vec{i})$ direction, $u^x(x,y)$, has two components – a uniform one and that one produced by rotation on angle $\theta_z^x(x)$:

$$u^x(x,y) = u^x(x) - \left(y - \frac{b}{2}\right) \cdot \theta_z^x(x) \tag{2d}$$

The similar 6 governing scalar parameters and relations can be introduced also for y-beam, Fig 1. They are related to the central line along *the* y direction, i.e. to $x = a/2$, and are the following:

– Vectorial concentrated force $\vec{F}^y(y)$ which consists of two scalar components: normal force $N^y(y)$ (acting in y direction) and shear force $L^y(y)$ (directed toward y-axis), Fig 1, i.e.:

$$\vec{F}^y(y) = N^y(y)\vec{j} + L^y(y)\vec{i} \tag{3a}$$

– Scalar bending moment $M_z^y(y)$ acting against the clockwise direction.

– Vectorial uniform displacement $\vec{\Pi}^y(y)$ which consists of two scalar components: normal displacement $v^y(y)$ (acting in y direction) and tangential one $u^y(y)$ (directed toward x-axis), i.e.:

$$\vec{\Pi}^y(y) = u^y(y)\vec{i} + v^y(y)\vec{j} \tag{3b}$$

– Scalar rotation angle $\theta_z^y(y)$ rotating against the clockwise direction (i.e. around the third z direction).

Note, that axial force $N^y(y)$ and bending moment $M_z^y(y)$ produce compressive axial stresses, $\sigma^y(x,y)$ at each side $y = const$:

$$\sigma^y(x,y) = \sigma_N^y(x) + \frac{(2x - a)}{a} \cdot \sigma_M^y(y) \tag{4a}$$

Where stress components are given by formulas:

$$\sigma_N^y(y)=\frac{N^y(y)}{ta};\ \sigma_M^y(y)=\frac{6\cdot M_z^y(y)}{ta^2} \tag{4b}$$

Shear force $L^y(y)$ produces uniform shear stress at this side:

$$\tau^y(y)=\frac{L^y(y)}{tb} \tag{4c}$$

Now consider the displacements along the side $y=const$. Everything is clear about the displacement $u^y(y)$ in $\vec{i}$ direction. In contrast, the displacement in $\vec{j}$ direction, $v^y(x,y)$, has two components – a uniform one and that one produced by rotation on angle $\theta_z^y(y)$:

$$v^y(x,y)=v^y(y)+\left(x-\frac{a}{2}\right)\cdot\theta_z^y(y). \tag{4d}$$

2.2. Physical equations (Gook's law)

Consider the axial deformations, ε, for both "beams". According to the definition, we can write them based on general expressions for axial displacements (2d) and (4d). Differentiating them, we have:

$$\varepsilon^x(x,y)=\frac{du^x(x,y)}{dx}=\frac{du^x(x)}{dx}-\left(y-\frac{b}{2}\right)\cdot\frac{d\theta_z^x(x)}{dx} \tag{5a}$$

$$\varepsilon^y(x,y)=\frac{dv^y(x,y)}{dy}=\frac{dv^y(y)}{dy}+\left(x-\frac{a}{2}\right)\cdot\frac{d\theta_z^y(y)}{dy}. \tag{5b}$$

Write the Gook's law (plane stress condition) with accounting for the adopted here signs for the stresses:

$$\varepsilon^x(x,y)=-\frac{1}{E}\left(\sigma^x(x,y)-\mu\sigma^y(x,y)\right). \tag{5c}$$

$$\varepsilon^y(x,y)=-\frac{1}{E}\left(\sigma^y(x,y)-\mu\sigma^x(x,y)\right). \tag{5d}$$

Substitute expressions for stresses (2a) and (4a) in (5c) and (5d). So, we get the following expressions for both beams:

$$\frac{du^x(x)}{dx}-\left(y-\frac{b}{2}\right)\cdot\frac{d\theta_z^x(x)}{dx}=-\frac{1}{E}\left(\left(\frac{N^x(x)}{tb}-\frac{\left(y-\frac{b}{2}\right)}{b}\times\right.\right.$$
$$\left.\left.\times\frac{12\cdot M_z^x(x)}{tb^2}\right)-\mu\left(\frac{N^y(y)}{ta}+\frac{\left(x-\frac{a}{2}\right)}{a}\cdot\frac{12\cdot M_z^y(y)}{ta^2}\right)\right) \tag{5e}$$

$$\frac{dv^y(y)}{dy}+\left(x-\frac{a}{2}\right)\cdot\frac{d\theta_z^y(y)}{dy}=-\frac{1}{E}\left(\left(\frac{N^y(y)}{ta}+\frac{\left(x-\frac{a}{2}\right)}{a}\times\right.\right.$$
$$\left.\left.\times\frac{12\cdot M_z^y(y)}{ta^2}-\mu\left(\frac{N^x(x)}{tb}-\frac{\left(y-\frac{b}{2}\right)}{b}\cdot\frac{12\cdot M_z^x(x)}{tb^2}\right)\right) \tag{5f}$$

Evidently, the deformations in the x-beam cannot depend on the independent variable y. So, take the values of "alien" parameters (in other words the y-dependent ones) in the fixed central point of the rectangular element, i.e. take $y=\frac{b}{2}$ for the x-beam, and $x=\frac{a}{2}$ for the y-beam. Thus, the following physical relations can be drawn out for x-beam:

$$\frac{du^x(x)}{dx}=-\frac{1}{E}\left(\frac{N^x(x)}{tb}-\mu\left(\frac{N^y(b/2)}{ta}+\frac{\left(x-\frac{a}{2}\right)}{a}\cdot\frac{12\cdot M_z^y(b/2)}{ta^2}\right)\right) \tag{6a}$$

$$\frac{d\theta_z^x(x)}{dx}=-\frac{1}{E}\left(\frac{12\cdot M_z^x(x)}{tb^3}\right). \tag{6b}$$

Similar relations are written for y-beam:

$$\frac{dv^y(y)}{dy}=-\frac{1}{E}\left(\frac{N^y(y)}{ta}-\mu\left(\frac{N^x(a/2)}{tb}-\frac{\left(y-\frac{b}{2}\right)}{b}\cdot\frac{12\cdot M_z^x(a/2)}{tb^2}\right)\right) \tag{6c}$$

$$\frac{d\theta_z^y(y)}{dy}=-\frac{1}{E}\left(\frac{12\cdot M_z^y(y)}{ta^3}\right). \tag{6d}$$

Now consider the relations for the shear stresses and deformations. The basic Gook's law in the elasticity theory is the following:

$$G\left(\frac{\partial v(x,y)}{\partial x}+\frac{\partial u(x,y)}{\partial y}\right)=-\tau(x,y) \tag{7a}$$

Where $\tau(x,y)$ is the shear stress, which is theoretically equal on both sides. In our approach, we discern between these stresses on the different sides, and this should be accounted for in our approach. So, law (7a) can be approximately satisfied if we rewrite the right side of (7a) as:

$$\left(\frac{\partial v^{x,e}(x)}{\partial x}+\frac{\partial u^{y,e}(y)}{\partial y}\right)=-\frac{1}{2G}\left(\frac{L^x(x)}{tb}+\frac{L^y(y)}{ta}\right) \tag{7b}$$

Here the upper index "e" means that a particular contribution is due to the consideration of the plane stress theory of elasticity. Evidently, we should break out this two-coordinate dependent relation into two independent ones:

$$\frac{\partial v^{x,e}(x)}{\partial x} = \gamma^x(x) = -\frac{1}{2Gbt} L^x(x). \quad (7c)$$

$$\frac{\partial u^{y,e}(y)}{\partial y} = \gamma^y(y) = -\frac{1}{2Gat} L^y(y). \quad (7d)$$

Equations (7c) and (7d) – are the approximate equations of the theory of elasticity. But here we consider the beams and operate additionally by the beam parameters. So, the deformation (7c) and (7d) are only a part of the whole beam deformation in the transverse direction. Another essential contribution is caused by the rotation of the central axis. So, we should supplement the elasticity deformation with the beam deformation:

$$\frac{\partial v^x(x)}{\partial x} = \theta_z^x(x) - \frac{1}{2Gbt} L^x(x). \quad (7e)$$

$$\frac{\partial u^y(y)}{\partial y} = -\theta_z^y(x) - \frac{1}{2Gat} L^y(y). \quad (7f)$$

2.3. Equilibrium equations

We cannot give the exact solution of the equilibrium equation within the element. It is impossible due to the consideration of the element as consisting of two almost independent beams. What can be done at the best is to preserve the integral equilibrium of the whole element. This will be done below. Furthermore, this integral equilibrium will be written in the differential form, i.e. the integration of the derived below differential equation will provide the global equilibrium of the element. Write out the equilibrium in the $\vec{i}$ direction according to the theory of elasticity:

$$\frac{\partial \sigma_x(x,y)}{\partial x} + \frac{\partial \tau_x^y(y,x)}{\partial y} = p_x. \quad (8a)$$

Consider that p_x is a constant outer distributed force in x-direction, multiply by the thickness t, and integrate it over the whole area of the element

$$\int_0^a dx \int_0^b \frac{\partial \sigma_x(x,y)}{\partial x} t dy + \int_0^b dy \int_0^a \frac{\partial \tau_x^y(y,x)}{\partial y} t dx = \int_0^b dy \int_0^a p_x dx \quad (8b)$$

$$\int_0^a \frac{\partial N^x(x)}{\partial x} dx + \int_0^b \frac{\partial L^y(y)}{\partial y} dy = ab \cdot p_x. \quad (8b)$$

Rewrite this equation in the differential form:

$$\frac{\partial N^x(x)}{b\partial x} + \frac{\partial L^y(y)}{a\partial y} = p_x. \quad (9a)$$

In a similar way derive the force equilibrium in the $\vec{j}$ direction:

$$\frac{\partial N^y(y)}{a\partial y} + \frac{\partial L^x(x)}{b\partial x} = p_y. \quad (9b)$$

Where p_y is an outer distributed force in y-direction. Similarly, write down the equilibrium of the rotation moment around the very small element with sides a and b:

$$\frac{\partial M_z^x(x)}{\partial x} a + L^x(x) a + \frac{\partial M_z^y(y)}{\partial y} b - L^y(y) b = 0. \quad (10a)$$

Break down this equation into two coordinate-independent equations:

$$\frac{\partial M_z^x(x)}{\partial x} + \frac{A_6}{a} + L^x(x) = 0. \quad (10b)$$

$$\frac{\partial M_z^y(y)}{\partial y} - \frac{A_6}{b} - L^y(y) = 0. \quad (10c)$$

Where we introduce the constant A_6. It envisages the interaction between the moments $M_z^x(x)$ and $M_z^y(y)$ within the element. Integrating equation (10b) by x, and equation (10c) by x and adding them, we will get the global moment equlibrity (10a).

3. Approximate analytical solutions

3.1. Rectangular element

The usual way of solution is applied here [1]. We start with the equilibrium equations. Then the physical equation will be solved, and at last, we give the ultimate solutions for geometrical equations.

Consider the force equilibrium. Take in (9a) and in (9b) that:

$$\frac{\partial L^y(y)}{a\partial y} = A_4; \quad \frac{\partial L^x(x)}{b\partial x} = A_5. \quad (11a)$$

Then from first equation (11a) and from equation (9b) we have the solution for forces in the y-beam:

$$L^y(y) = L_0^y + A_4 a y. \quad (11b)$$

$$N^y(y) = N_0^y + p_y a y - A_5 a y. \quad (11c)$$

From the second equation of (11a) and the equation we get for x-beam:

$$L^y(y) = L_0^y + A_4 a y. \quad (11d)$$

$$N^x(x) = N_0^x + p_x b x - A_4 b x. \quad (11e)$$

The values of moments are derived by integration of (10b) and (10c):

$$M_z^x(x) = M_{z,0}^x - L_{y,0}^x x - A_5 b\frac{x^2}{2} - \frac{A_6}{a}x\,. \qquad (12a)$$

$$M_z^y(y) = M_{z,0}^y + L_{x,0}^y y + A_4 a\frac{y^2}{2} + \frac{A_6}{b}y\,. \qquad (12b)$$

The formulas for angles of rotation for both "beams" are derived from physical dependences (6b) and (6d) and solutions for moments (12a) and (12b):

$$\theta_z^x(x) = \theta_{z,0}^x - \frac{12}{Etb^3}\left(M_{z,0}^x x - L_{y,0}^x\frac{x^2}{2} - A_5\frac{bx^3}{6} - \frac{A_6}{a}\frac{x^2}{2}\right) \qquad (13a)$$

$$\theta_z^y(y) = \theta_{z,0}^y - \frac{12}{Eta^3}\left(M_{z,0}^y y + L_{x,0}^y\frac{y^2}{2} + A_4\frac{ay^3}{6} + \frac{A_6}{b}\frac{y^2}{2}\right) \qquad (13b)$$

The last step is to obtain the solution for displacement.

Consider *x*-beam. Axial displacement is derived by integration of (6a), and tangential displacement – by (7e):

$$u^x(x) = u_0^x - \frac{1}{E}\left(\frac{N_0^x x + \left(p_x\frac{bx^2}{2} - A_4\frac{bx^2}{2}\right)}{tb}\right) + \\ + \frac{\mu}{E}\left(x\frac{N_0^y + p_y\frac{ba}{2} - A_5\frac{ba}{2}}{ta} + \frac{6x(x-a)}{ta^3}\left(M_{z,0}^y + L_{x,0}^y\frac{b}{2} + A_4\frac{ab^2}{8} + A_6\frac{1}{2}\right)\right) \qquad (14a)$$

$$v^x(x) = v_0^x + \theta_{z,0}^x x - \frac{12}{Etb^3}\left(M_{z,0}^x\frac{x^2}{2} - L_{y,0}^x\frac{x^3}{6} - \right. \\ \left. - A_5\frac{bx^4}{24} - \frac{A_6}{a}\frac{x^3}{6}\right) - \frac{1}{2Gbt}\left(L_{y,0}^x x + A_5\frac{bx^2}{2}\right). \qquad (14b)$$

Now consider *y*-beam. Axial displacement is derived by integration of (6c), and tangential one – by (7f):

$$v^y(y) = v_0^y - \frac{1}{E}\left(\frac{N_0^y y + \left(p_y\frac{ay^2}{2} - A_5\frac{ay^2}{2}\right)}{ta}\right) + \\ + \frac{\mu}{E}\left(\left(y\frac{N_0^x + p_x\frac{ba}{2} - A_4\frac{ba}{2}}{tb} - \frac{6y(y-b)}{tb^3}\left(M_{z,0}^x - L_{y,0}^x\frac{a}{2} - A_5\frac{ba^2}{8} - A_6\frac{1}{2}\right)\right)\right) \qquad (14c)$$

$$u^y(y) = u_0^y - \theta_{z,0}^y y + \frac{12}{Eta^3}\left(M_{z,0}^y\frac{y^2}{2} + L_{x,0}^y\frac{y^3}{6} - \right. \\ \left. + A_4\frac{ay^4}{24} + \frac{A_6}{b}\frac{y^3}{6}\right) - \frac{1}{2Gat}\left(L_{x,0}^y y + A_4\frac{ay^2}{2}\right). \qquad (14d)$$

The above 12 equations in this subchapter starting from (11b) and up to the last one (14d) give the solutions for all 12 parameters (6+6) in each point of either beam.

The unknown constants A_4, A_5, and A_6 are extracted from consideration by employing the continuity conditions at the center of the rectangular element. These conditions provide equality of two independent displacements and one angle of rotation. Write the continuity of displacements. They are evident:

$$u^x\left(\frac{a}{2}\right) = u^y\left(\frac{b}{2}\right) \qquad (15a)$$

$$v^x\left(\frac{a}{2}\right) = v^y\left(\frac{b}{2}\right). \qquad (15b)$$

The relationship between the angles of rotations is not so evident as for displacements. Provided that there is no shear deformation then the angles of rotation of both sides should be the same (rotation of the body as a rigid):

$$\theta_z^x\left(\frac{a}{2}\right) = \theta_z^y\left(\frac{b}{2}\right).$$

Yet this is the wrong condition because of the shear deformation (7c) and (7d). The action of $L^x(x)$ rotates the lower side θ_z^y on an additional angle $\gamma^x(x)$ and the action of $L^y(y)$ rotates the left side θ_z^x on an additional angle $-\gamma^y(y)$. Accounting for this additional shear deformation the relations between the angles will be the following:

$$\theta_z^x\left(\frac{a}{2}\right) + \gamma^x(a/2) = \theta_z^y\left(\frac{b}{2}\right) - \gamma^y(b/2). \qquad (15c)$$

3.2. Right triangular element

The element with the right-upper hypothenuse is shown in Fig. 2. It serves for the geometry adjustment at the real body boundaries. It has three sides. Introduce the angle φ between the lower leg and hypotenuse. We have the following dependencies between the sides of the triangle:

$$a\cdot tg\varphi = b\,,\ l\cdot cos\varphi = a\,,\ l\cdot sin\varphi = b \qquad (16a)$$

$$\vec{l} = \vec{b} - \vec{a}\,,\ \vec{a} = \vec{i}\cdot a\,,\ \vec{b} = \vec{j}\cdot b\,. \qquad (16b)$$

Write the unit tangent vector, $\vec{s}$, to the inclined side, evidently:

$$\vec{s} = \frac{\vec{l}}{l} = \frac{\vec{b} - \vec{a}}{\sqrt{a^2 + b^2}}\,. \qquad (16c)$$

The normal vector on the hypotenuse is $\vec{n}$ (directed outward) and the tangent vector is $\vec{s}$. From Fig. 2, it is evident that:

$$\vec{n} = \vec{i}sin\varphi + \vec{j}cos\varphi\,,\ \vec{s} = -\vec{i}cos\varphi + \vec{j}sin\varphi\,. \qquad (16d)$$

Or

$$\vec{i} = \vec{n}sin\varphi - \vec{s}cos\varphi\,,\ \vec{j} = \vec{s}sin\varphi + \vec{n}cos\varphi\,. \qquad (16e)$$

Our solution for the right triangular element will be based on the above solution for the rectangular element. Yet in this case, there is no necessity to introduce the auxiliary constants A_4, A_5, and A_6. They are taken to be zero because the interchange between the forces occurs just on the hypothenuse.

The x-beam is considered to have the width b as usual. But its length now is taken to be $a/2$. So, all parameters in it are calculated from the above formulas (11d), (11e), (12a), (13a), (14a) and (14b). The y-beam is considered to have the width a. But its length now is taken to be $b/2$. So, all parameters in it are calculated from the formulas (11b), (11c), (12b), (13b), (14c) and (14d).

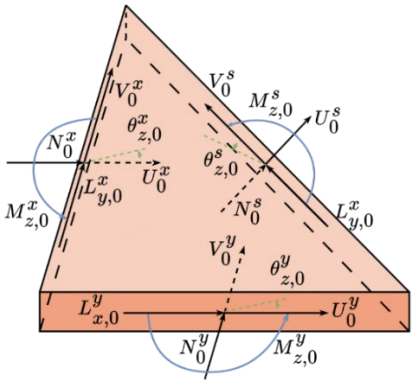

Fig 2. The scheme and designations for a right triangular element with right-upper hypothenuse

Consider the side l and prescribe that it is an outlet side. On this side, we also have 6 parameters that characterize any beam side. The vector of forces on this side, $\vec{F}^{\varphi}$, can be presented as:

$$\vec{F}^{\varphi} = F^n\vec{n} + F^s\vec{s}\,, \tag{17a}$$

where F^n is the force projection in the direction of $\vec{n}$, and F^s is the projection along $\vec{s}$. The vector of displacement $\vec{\Pi}^{\varphi}$ can be written as:

$$\vec{\Pi}^{\varphi} = \Pi^n\vec{n} + \Pi^s\vec{s}\,, \tag{17b}$$

where Π^n is the force projection in the direction of $\vec{n}$, and Π^s is the projection along $\vec{s}$. This side also is characterized by the bending moment M_z^{φ} and the angle of rotation θ_z^{φ}.

Compile 9 scalar equations within this element. The two first equations can be derived from the condition that the sum of vectorial inlet forces in point O, Fig. 2, should be equal to outlet force (17a), i.e.:

$$N^x\left(\frac{a}{2}\right)\vec{i} + L^x\left(\frac{a}{2}\right)\vec{j} + N^y\left(\frac{b}{2}\right)\vec{j} + L^y\left(\frac{b}{2}\right)\vec{i} = F^n\vec{n} + F^s\vec{s}\,. \tag{18a}$$

Where from with accounting for vectorial dependences (16e):

$$F^n = N^x\left(\frac{a}{2}\right)\sin\varphi + L^x\left(\frac{a}{2}\right)\cos\varphi + N^y\left(\frac{b}{2}\right)\cos\varphi + L^y\left(\frac{b}{2}\right)\sin\varphi \tag{18b}$$

$$F^s = -N^x\left(\frac{a}{2}\right)\cos\varphi + L^x\left(\frac{a}{2}\right)\sin\varphi + N^y\left(\frac{b}{2}\right)\sin\varphi - L^y\left(\frac{b}{2}\right)\cos\varphi \tag{18c}$$

The next 4 equations are the equality of vectorial displacements as those pertained to: 1) x- beam in point $\frac{a}{2}$; 2) - beam in point $\frac{b}{2}$; 3) to the side φ. Thus we have for projections on vector $\vec{s}$:

$$-u^x\left(\frac{a}{2}\right)\cos\varphi + v^x\left(\frac{a}{2}\right)\sin\varphi = -u^y\left(\frac{b}{2}\right)\cos\varphi + v^y\left(\frac{b}{2}\right)\sin\varphi = \Pi^s\,. \tag{19a}$$

$$u^x\left(\frac{a}{2}\right)\sin\varphi + v^x\left(\frac{a}{2}\right)\cos\varphi = u^y\left(\frac{b}{2}\right)\sin\varphi + v^y\left(\frac{b}{2}\right)\cos\varphi = \Pi^n\,. \tag{19b}$$

The requirement of equality of angles of rotation in the central point O, Fig. 2, pertained to three different sides, leads to two additional equations:

$$\theta_z^x\left(\frac{a}{2}\right) + \gamma^x\left(\frac{a}{2}\right) = \theta_z^y\left(\frac{b}{2}\right) - \gamma^y\left(\frac{b}{2}\right) = \theta_z^x\left(\frac{a}{2}\right) + \gamma^x\left(a/2\right) = \theta_z^S\left(\frac{b}{2}\right) - \gamma^s\left(\frac{a}{2},\frac{b}{2}\right). \tag{19c}$$

The condition of equality of the sum of input moment to the sum of output moments leads to the last nineth equation within the right rectangular element:

$$M_z^x\left(\frac{a}{2}\right) + M_z^y\left(\frac{b}{2}\right) = M_z^{\varphi}\,. \tag{20b}$$

Remind, that solutions for x- and y- beams are derived from subchapter 3.1 where all three constants A_4, A_5, A_6 and A6 are taken to be zero. Similarly, the equations can be written for 3 other cases of placement of the hypothenuse in the right triangular elements.

4. Examples of calculations

To spare the place we omit here the description of the organization of the calculation process. It is described in detail in works [1]–[4] and technically it is based on the transfer matrix method, TMM [23].

Consider two typical examples used in the substantiation of the efficiency of the numerical methods [24]–[26].

4.1. Cantilever beam like the rectangular CFFF plate

First, let us consider the simplest case - a rectangular plate stretched along one X-axis three sides of which are free, *F*, and the left side is clamped, C, Fig. 3. Let's study to what extent the elongation and the number of elements affect the quality of the obtained results. Fix the linear dimensions of the element as $l_x = 20$, $l_y = 1$, so this large ratio allows us to consider the plate as a beam, especially in its central sections. The right side is loaded with a unit evenly distributed shear force along the *x*-axis, Fig. 3.

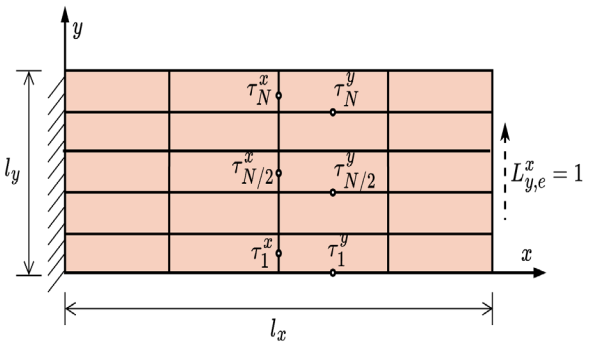

Fig 3. Cantilever beam-like CFFF plate

A theoretical beam-like solution for normal stress $\sigma^x_*(y)$ and shear stress $\tau^x_*(y)$ in the central section ($x = 10$) can be obtained readily by using the following formula:

$$\sigma^x_*(y) = 10 \cdot \frac{6(y-0.5)}{0.5} = 60 \cdot (2y-1) \qquad (21a)$$

$$\tau_*(y) = 1.5\left(1-(2y-1)^2\right). \qquad (21b)$$

The first comparison will be made on the center line of the vertical line at $x = 10$. According to (21b), along this line, τ_* varies parabolically, and has a maximum of $\tau_* = 1.5$ at $y = l_y/2 = 0.5$. The stress σ^x_* varies linearly, from 60 to –60, respectively, Fig. 4.

Note that the MMS solution results in τ^x_m values somewhat averaged along the sides of the corresponding elements. And since the vertical amount of elements, N, is assumed to be small, it is more appropriate to transform shear stresses (21b) into the averaged values of $\tau_{m,avg}$, where m is the particular element number in the vertical direction, Fig. 3.

$$\tau_{m,avg} = N\int_{\frac{m-1}{N}}^{\frac{m}{N}} 1.5\left(1-(2y-1)^2\right)dy = $$

$$= 1.5\left(\frac{4m-2}{N} - \frac{4\left(3m^2-3m+1\right)}{3\cdot N^2}\right). \qquad (22a)$$

For example, when N is uneven, then the averaged shear stress in the central element, $\tau_{c,avg}$, is calculated for $m = (N+1)/2$:

$$\tau_{c,avg} = 1.5\left(1-\frac{1}{3\cdot N^2}\right). \qquad (22b)$$

Now let us calculate stress values using MMS. We start with a 2×1 base grid, where $M = 2$ elements along the x-axis, and $N = 1$ along y-axis. We will check the calculated central, $\tau^x_{m=N/2,}$ and the edge values of $\tau^x_{m=N,}$ and the edge values of $\tau^x_{m=1}$ and the edge values of σ^x_N, and compare them with the theoretical averaged central values of $\tau_{c,avg}$ and the edge values of $\tau_{1,avg}$, Table 1. Evidently, the results for σ^x_N calculated by the formula (2a) with (2b) are very good notwithstanding the mesh refinement, nor from the a/b ratio. In some cases, for a small number of elements in *the x*-direction (*M*) and a very large a/b ratio, the results are a little smaller than the theoretical ones.

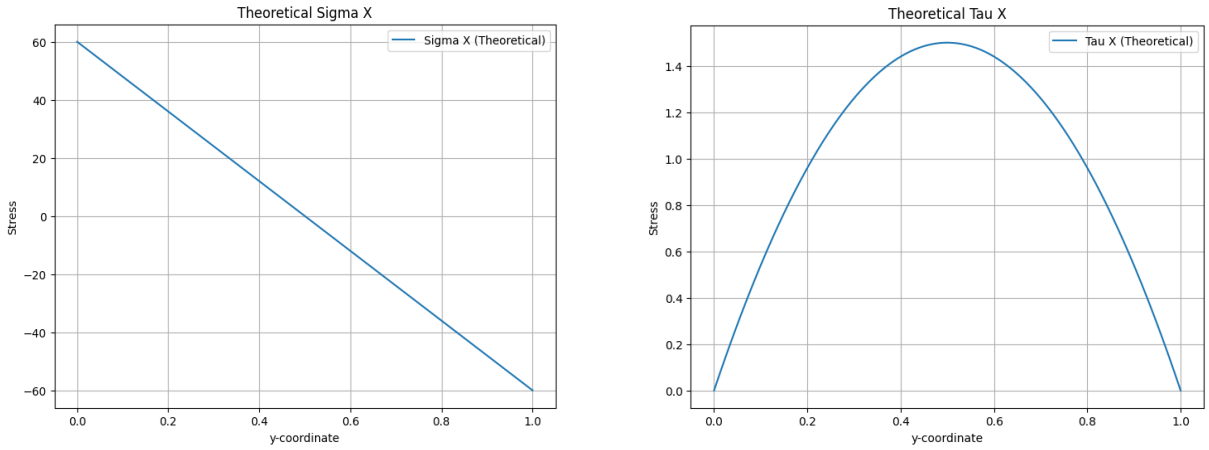

Fig 4. Theoretical stresses for beam-like CFFF plate

Table 1. Comparison of τ^x results for beam-like CFFF plate depending on the grid and aspect ratio

N	M	a/b	$\tau^x_{m=N/2}$	$\tau_{c,\,avg}$	$\tau^x_{m=1}$	$\tau_{1,\,avg}$	σ^x_N
1	2	10	1	**1**	1	**1**	60
	6	3.33	1		1		60
3	2	30	1.0061	**1.44**	0.997	**0.78**	59.9565
	8	7.5	1.248		0.876		60.0132
	32	1.875	1.3484		0.8258		60.0000
5	2	50	1.0024	**1.48**	0.9976	**0.52**	59.9455
	16	6.25	1.3132		0.6887		60.0005
	64	1.562	1.4346		0.5729		60.0000
11	2	110	1.0005	**1.5**	0.9992	**0.26**	59.9604
	32	6.875	1.3576		0.4834		60.0000
	128	1.7188	1.4799		0.3047		60.0000
21	8	52.5	1.0346	**1.5**	0.9415	**0.14**	59.8996
	64	6.5625	1.4246		0.3238		60.0000
	256	1.64	1.495		0.1645		60.0000

Table 2. Comparison of τ^y results for beam-like CFFF plate depending on the mesh and aspect ratio

$M \times N$	a/b	$\tau^y_1 \,\vert\tau_*(y=0)$	$\tau^y_m \,\vert\tau_*(y=0.5)$	$\tau^y_{m+1} \,\vert\tau_*(y=0.5+\frac{1}{N})$
2×3	30	1.3334 | 1.3333	1.3334 | 1.3333	0.0000 | 0.0000
8×3	7.5	1.3333 | 1.3333	1.3333 | 1.3333	0.0000 | 0.0000
2×5	50	0.9600 | 0.9600	1.4400 | 1.4400	0.9600 | 0.9600
16×5	6.25	0.9600 | 0.9600	1.4400 | 1.4400	0.9600 | 0.9600
2×11	110	0.4959 | 0.4959	1.4876 | 1.4876	1.3885 | 1.3884
32×11	6.875	0.4959 | 0.4959	1.4876 | 1.4876	1.3884 | 1.3884
4×31	155	0.1873 | 0.1873	1.4984 | 1.4984	1.4859 | 1.4860

As to τ^x values, they require a larger number of N and M refinement to become accurate and the ratio of a/b needs to be close to 1.

Comparison of the τ^x results is complicated by the fact that they are integrally averaged along the sides of the corresponding elements. It is worth recalling that MMS does not use the law of equality of the shear stresses. It is of interest to calculate and compare the values of shear stress along the horizontal sides of the elements, τ^y, as indicated in Fig. 3. And compare them with the values obtained through (21b), for different aspect ratios and mesh densities, Table 2.

Although our method do not explicitly equal τ^x and τ^y, their values become very similar when the grid is sufficiently dense. This can be easily seen in Fig. 5, where the grid is taken as $M = 256$, $N = 11$.

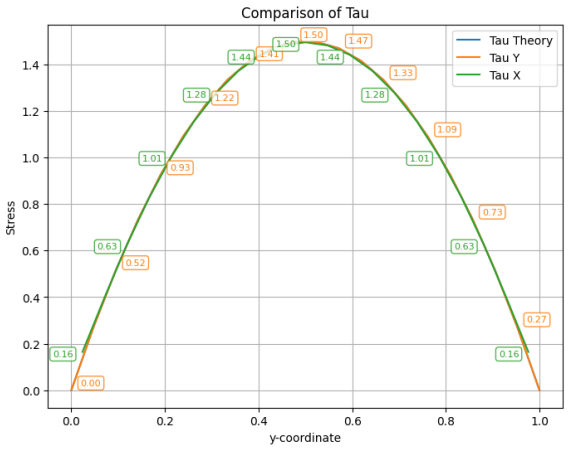

Fig 5. Tau comparison for a dense grid

4.2. Infinite plate with a circular cutout

Now let's move on to a much more complicated geometry. Consier a rectangular plate with infinitely long sides, with a circular cutout with a radius a_c in its center. The origin of the coordinates is at the center of the plate. A unit force is applied to the right side along the *x*-axis. An analytical solution to this problem is proposed is given, among others in [26]. Thus, the stresses are expressed using the following formulas:

$$\sigma^x = T - T\frac{a_c^2}{r^2}\left(\frac{3}{2}cos2\theta + cos4\theta\right) + T\frac{3a^4}{2r^4}cos4\theta, \quad (23a)$$

$$\sigma^y = -T\frac{a_c^2}{r^2}\left(\frac{1}{2}cos2\theta - cos4\theta\right) - T\frac{3a^4}{2r^4}cos4\theta, \quad (23b)$$

$$\tau^{xy} = -T\frac{a_c^2}{r^2}\left(\frac{1}{2}sin2\theta + sin4\theta\right) + T\frac{3a^4}{2r^4}sin4\theta, \quad (23c)$$

where

$$r = \sqrt{x^2 + y^2},\ sin2\theta = \frac{2xy}{x^2 + y^2},\ cos2\theta = \frac{x^2 - y^2}{x^2 + y^2}, \quad (23d)$$

$$sin4\theta = \frac{4xy\left(x^2 - y^2\right)}{\left(x^2 + y^2\right)^2},\ cos4\theta = \frac{\left(x^2 - y^2\right)^2 - 4x^2y^2}{\left(x^2 + y^2\right)^2}. \quad (23e)$$

The maximum stress concentration occurs at $(a_c, 0)$, where $\sigma_x = 3T$.

For calculations, let us consider the finite part of this plate with radius a_c. Namely, the right upper quarter of a figure with finite length l_x and height l_y, Fig. 6. We are left with a cutout in the form of a quarter circle of radius a_c. To qualitatively describe a quarter circle let us place N_c points on it. Then, place triangular elements on the boundary so that the points on the arc are their vertices.

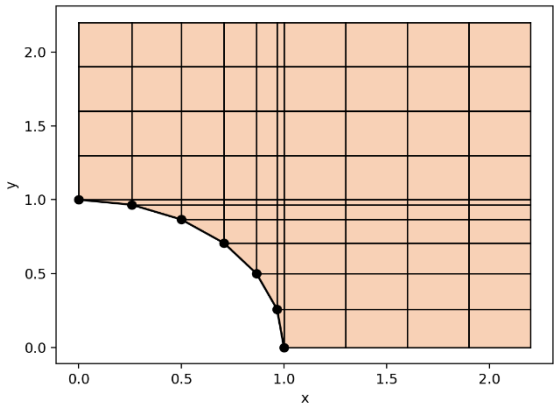

Fig. 6. Plate with a circular cutout $(N_c = 7)$

Within this geometry, we need to set the boundary conditions correctly to model an infinite body. The boundary conditions for $x = 0$ and $y = 0$ are simple symmetry conditions: $U_0^x = \theta_0^x = L_0^x = 0$ for the left side and $V_0^y = \theta_0^y = L_0^y = 0$ for the bottom side, respectively. The cutout boundary is free, so we set the force components there to zero.

The situation is more complicated with the right and upper bounds. We need to set on these boundaries the loads described in (23a-c). However, we operate with forces and moments distributed along the sides of the elements, while the analytical formulas specify stresses pointwise.

Let us consider the right boundary of the lower right element as an example. For calculating the N^x and L^x, the equations (23a-b) simply need to be integrated along the right side, (24a-b).

$$N^x = \int_0^b \sigma^x\left(x = l_x\right)dy, \quad (24a)$$

$$L^x = \int_0^b \tau^{xy}\left(x = l_x\right)dy. \quad (24b)$$

Among other things, MMS allows moment loads to be applied as boundary conditions. The moments have maximum values at the edge points of the element side. Maximum negative at the bottom $(y = 0)$, and maximum positive at the top $(y = b)$. That is, it is necessary to integrate σ^x while multiplying each integration segment by the distance to the center of the side, $b_c(y)$, considering the sign, (25a).

$$M^x = \int_0^b \sigma^x\left(x = l_x\right)\left(y - 0.5\right)dy. \quad (24c)$$

The analogous approach is also applied to the upper side ($y = l_y$).

Suppose we have a plate with length $l_x = 3$, height $l_y = 2$, and radius of the cutout circle $a_c = 1$. Let's apply for it the base mesh $M = N = 71$, and describe the circle with $N_c = 23$ points. We present the results along the horizontal and vertical lines of greatest interest to us, Fig. 7.

From the results, we can see that MMS allows us to describe complex geometry using a small mesh of elements. For more clarity, numerical results at the points of greatest difference are given, Table 3.

Table 3. Comparison of results for an infinite plate with a circular cutout

l_x, l_y	$M \times N$ N_c	$\sigma^x(0,1)$	$\sigma^y(1,0)$	$\tau^{xy}(1,1)$
3, 2	71, 71 23	3.0816	–0.8868	–0.25
Analytical		3	–1	–0.25

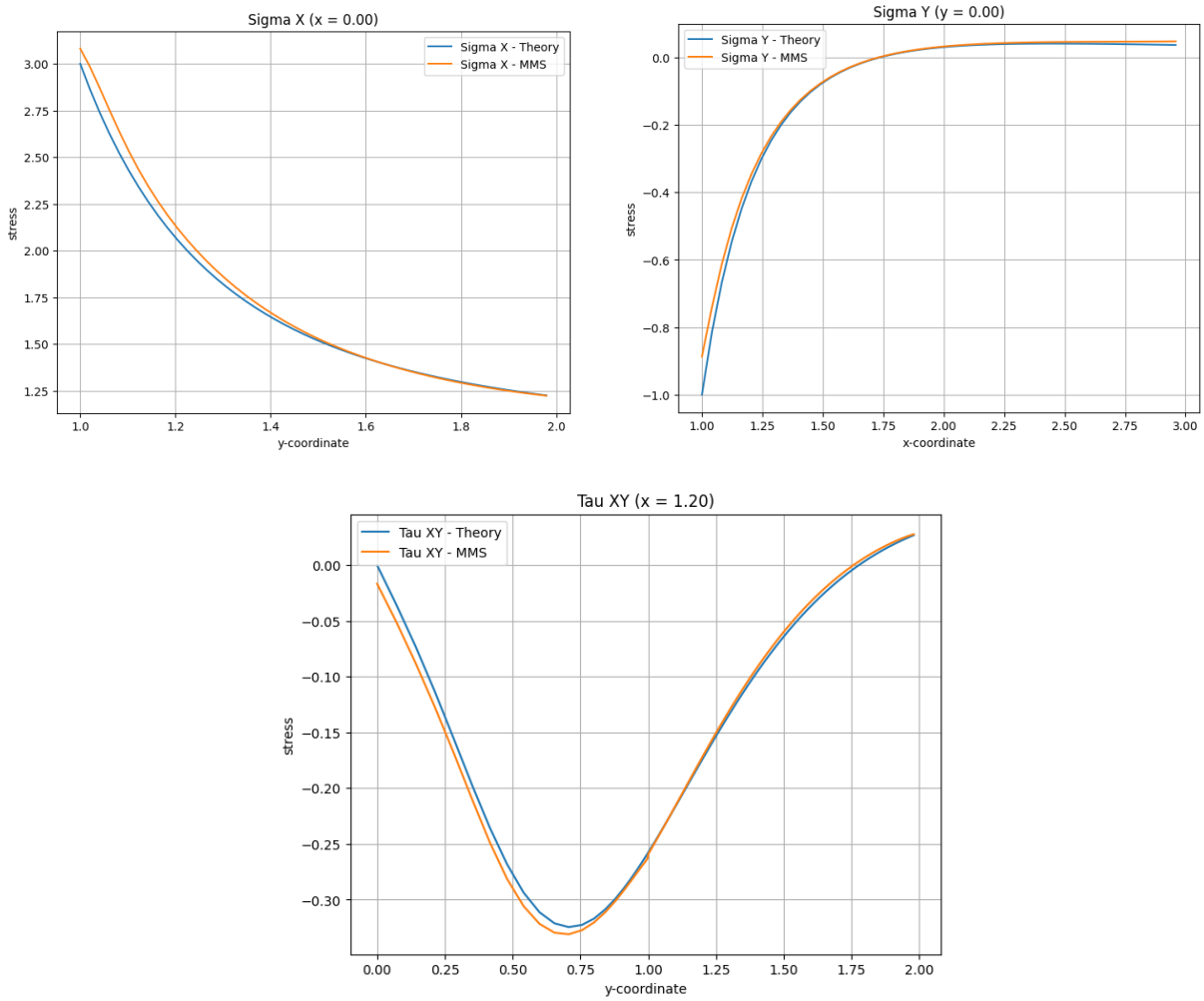

Fig 7. Comparison of results for an infinite plate with a circular cutout

Conclusion

The method of the matched section has been proven to be an effective numerical technique for solving the complicated problems of mathematical physics formulated through partial differential equations. MMS is a new variant of the FEM and contains all its principal features – meshing on finite elements, the substitution of the differential dependences by an algebraical one for each element, compilation of equations, and solution of the global matrix. Yet its main unique feature is the substitution of the partial differential equations by the ordinary ones with subsequent exact or approximate solution of them. This allows to accurately account for all known 1D behavioral peculiarities and avoid all unwanted effects related, for example, with shear, membrane, and volume locking. The significance of the present paper consists in:

1. For the first time it considers the 2D plane body problem of the elasticity by the MMS. Instead of the hypothesis of equality of shear stress the equation of the moment equilibrium is accounted for each element.

2. For the first time in MMS application the deformable right triangular element is formulated. It allows to accurately treat any geometrical peculiarities of the boundaries.

3. In contrast to traditional FEM each MMS element exactly satisfies the force equilibrium in either of two directions as well as the moment equilibrium. Thus, the equilibrium is fulfilled exactly for the whole body as well.

4. Numerical verification is performed for the cantilever beam considered as the plain body and for the infinite body with the circular hole. It is shown that even a relatively small number of elements (coarse meshing) is able to provide the desired accuracy. The shear stresses on all sides of the inner elements are very close, so the requirement of their equality is principally satisfied.

References

[1] I. Orynyak and K. Danylenko, "Method of matched sections as a beam-like approach for plate analysis," *Finite Elements in Analysis and Design*, 230, 104103, 2024, doi: 10.1016/j.finel.2023.104103.

[2] I. Orynyak and K. Danylenko, "Method of matched sections in application to thin-walled and Mindlin rectangular plates," *Mechanics and Advanced Technologies*, Vol. 7, No. 2, 2023, doi: 10.20535/2521-1943.2023.7.2.277341.

[3] I. Orynyak, A. Tsybulnyk, K. Danylenko, A. Oryniak and S. Radchenko, "Timestep-dependent element interpolation functions in the method of matched sections on the example of heat conduction problem," *Journal of Computational and Applied Mathematics*, 456, 116222, 2025, doi: 10.1016/j.cam.2024.116222.

[4] I. Orynyak, A. Tsybulnyk and K. Danylenko, "Spectral realization of the method of matched sections for thin plate vibration," *Archive of Applied Mechanics.* Accepted for publication.

[5] A. Hrennikoff, "Solution of Problems of Elasticity by the Framework Method," *Journal of Applied Mechanics*, Vol. 8, No. 4, Dec. 1941, doi: 10.1115/1.4009129.

[6] M. J. Turner, R. W. Clough, H. C. Martin and L. J. Topp, "Stiffness and deflection analysis of complex structures," *Journal of the Aeronautical Sciences*, 23(9), pp. 805–823, 1956, doi: 10.2514/8.3664.

[7] O. C. Zienkiewicz, R. L. Taylor and J. Z. Zhu, *The finite element method: its basis and fundamentals*, Elsevier, 2005.

[8] V. E. B. İ. L. Haktanir and E. Kiral, "Statical analysis of elastically and continuously supported helicoidal structures by the transfer and stiffness matrix methods," *Computers & Structures*, 49(4), pp. 663–677, 1993, doi: 10.1016/0045-7949(93)90070-T.

[9] F. N. Gimena, P. Gonzaga and L. Gimena, "Stiffness and transfer matrices of a non-naturally curved 3D-beam element," *Engineering Structures*, 30(6), pp. 1770–1781, 2008, doi: 10.1016/j.engstruct.2007.10.012.

[10] H. Zhong, Z. Liu, H. Qin and Y. Liu, "Static analysis of thin-walled space frame structures with arbitrary closed cross-sections using transfer matrix method," *Thin-Walled Structures*, 123, pp. 255–269, 2018, doi: 10.1016/j.tws.2017.11.018.

[11] Y. H. Cao, G. M. Liu and Z. Hu, "Vibration calculation of pipeline systems with arbitrary branches by the hybrid energy transfer matrix method," *Thin-Walled Structures*, 183, 110442, 2023, doi: 10.1016/j.tws.2022.110442.

[12] Y. Goto, Y. Morikawa and S. Matsuura, "Direct Lagrangian nonlinear analysis of elastic space rods using transfer matrix technique," *Proc. of JSCE, Struct. Eng./Earthquake Eng*, 5(1), 1986.

[13] I. V. Orynyak and S. A. Radchenko, "A mixed-approach analysis of deformations in pipe bends. Part 3. Calculation of bend axis displacements by the method of initial parameters," *Strength of materials*, 36, pp. 463–472, 2004, doi: 10.1023/B:STOM.0000048394.98411.4f.

[14] E. Tufekci, U. Eroglu, and S. A. Aya, "A new two-noded curved beam finite element formulation based on exact solution," *Engineering with computers*, 33, pp. 261–273, 2017, doi: 10.1007/s00366-016-0470-1.

[15] Y. Yamada, Y. Ezawa, "On curved finite elements for the analysis of circular arches," *International Journal for Numerical Methods in Engineering*, 11(11), pp. 1635–1651, 1977, doi: 10.1002/nme.1620111102.

[16] K. Fumio, "On the validity of the finite element analysis of circular arches represented by an assemblage of beam elements," *Computer Methods in Applied Mechanics and Engineering*, 5(3), pp. 253–276, 1975, doi: 10.1016/0045-7825(75)90001-8.

[17] E. Wilson, *Three Dimensional Static and Dynamic Analysis of Structures*, Computers and Structures, Inc.2000.

[18] J. M. de Almeida and E. A. Maunder, *Equilibrium finite element formulations,* John Wiley & Sons, 2017.

[19] J. M. de Almeida and J. Reis, "An efficient methodology for stress-based finite element approximations in two-dimensional elasticity," *International Journal for Numerical Methods in Engineering*, 121(20), pp. 4649–4673, 2020, doi: 10.1002/nme.6458.

[20] K. Olesen, B. Gervang, J. N. Reddy and M. Gerritsma, "A higher-order equilibrium finite element method," *International journal for numerical methods in engineering*, 114(12), pp. 1262–1290, 2018, doi: 10.1002/nme.5785.

[21] S. Ham and K. J. Bathe, "A finite element method enriched for wave propagation problems," *Computers & structures*, 94, pp. 1–12, 2012, doi: 10.1016/j.compstruc.2012.01.001.

[22] F. Parrinello and G. Borino, "Hybrid equilibrium element with high-order stress fields for accurate elastic dynamic analysis," *International Journal for Numerical Methods in Engineering*, 122(21), pp. 6308–6340, 2021, doi: 10.1002/nme.6793.

[23] I. Orynyak, *Calculation of complex systems by transfer matrix method*, Kyiv "I. Sikorsky Kyiv Polytechnical Institute", 324 p. ISBN978-617-7619-47-4, 2022.

[24] R. H. Macneal and R. L. Harder, "A proposed standard set of problems to test finite element accuracy," *Finite elements in analysis and design*, 1(1), pp. 3–20, 1985, doi: 10.1016/0168-874X(85)90003-4

[25] K. M. Rao and U. Shrinivasa, A set of pathological tests to validate new finite elements. *Sadhana*, *26*, 549-590.2001, doi: 10.1007/BF02703459

[26] Hematiyan, M. R., Arezou, M., Dezfouli, N. K., & Khoshroo, M. (2019). Some remarks on the method of fundamental solutions for two-dimensional elasticity. *Computer Modeling in Engineering & Sciences*, *121*(2), pp. 661–686, doi: 10.32604/cmes.2019.08275.

Числовий аналіз задачі статики пружного плоского тіла методом узгоджених січень

К. Даниленко[1] • І. Ориняк[1]

[1] *КПІ ім. Ігоря Сікорського, Київ, Україна*

Анотація. *Стаття продовжує цикл авторських робіт з розробки принципово нового варіанту методу скінченних елементів МСЕ для вирішення різноманітних задач математичної фізики, а саме методу узгоджених січень МУС. Тут розглядається пружне плоске тіло при статичному навантаженні. Як і в МСЕ, все тіло розбивається на дрібні елементи, переважно, прямокутної форми. Основна особливість методу полягає у введенні набору основних параметрів, які залежать лише від однієї координатної змінної, тобто від x або y. Таким чином, будь-яке диференційне рівняння рівноваги з двома частинними похідними по x або y розбивається на два відносно простих рівняння по відношенню лише до однієї незалежної змінної. Це призводить до введення однієї додаткової константи, яка показує взаємообмін між цими двома рівняннями. Введені константи можна вивести з рівняння неперервності кінематичних параметрів у центрі кожного елемента. Основними, наприклад, залежними від x параметрами є:* $v^x(x)$ *та* $u^x(x)$ *переміщення у вертикальному (y-) і горизонтальному (x-) напрямках відповідно; нормальна* $N^x(x)$ *і тангенціальна (зсувна)* $L^x(x)$ *сили в x -напрямку та y- напрямках відповідно; і згинальний момент* $M^x(x)$ *і кут повороту* $\theta(x)$*. Подібні параметри встановлюються і для напрямку y. На основі методології методу початкових параметрів встановлюється аналітична залежність у вигляді матриці звязку між цими параметрами в будь-якій точці x або y та параметрами на нижній та/або лівій межі елемента. Для обробки похилих і криволінійних границь виведено прямокутний трикутний елемент як окремий вироджений випадок прямокутного елемента. Отримана система лінійних рівнянь формуються для невідомих значень усіх параметрів, заданих на межі всіх елементів. Ефективність і чудова точність МУС продемонстрована на класичних прикладах згинання довгого прямокутного тіла (балкова геометрія) і розтягування на нескінченності 2D тіла з маленьким круговим отвором.*

Ключові слова: *Метод узгоджених січень, метод початкових параметрів, пружне плоске тіло, трикутний елемент, граничні умови, нескінчена пластина з круглим отвором.*